Springer Proceedings in Mathematics & Statistics

Emmanuel Franck
Jürgen Fuhrmann
Victor Michel-Dansac
Laurent Navoret *Editors*

Finite Volumes for Complex Applications X—Volume 2, Hyperbolic and Related Problems

FVCA10, Strasbourg, France, October 30, 2023–November 03, 2023

Springer

A Low Mach Number Two-Speed Relaxation Scheme for Ideal MHD Equations

Claudius Birke and Christian Klingenberg

Abstract In this work we apply the two-speed relaxation technique to a relaxation system for the compressible ideal magnetohydrodynamic (MHD) equations. We show that the resulting approximate Riemann solver reduces the dissipation in the low Mach number regime and can thus generate accurate solutions in this regime even on coarse grids. These findings are supported by numerical results.

Keywords Finite volume methods · Relaxation methods · Approximate Riemann solver · Low Mach number regime

1 Introduction

In practical applications such as the simulation of gas flows in the interior of stars, flows with large scale differences can occur. One example is the low sonic Mach number regime, in which the sound speed is much higher than the speed of the fluid flow. Numerically, for standard finite volume methods two difficulties arise in the low Mach number regime: excessive dissipation and a restrictive CFL condition. Basically, there are two strategies in the literature to deal with these challenges:

1. (a) Introduce a low Mach number fix in the numerical flux function to reduce the dissipation and (b) use an implicit time integration to overcome the restrictive CFL condition [10, 11].
2. Perform a splitting into convective and acoustic parts and solve the acoustic parts implicitly [7, 8].

C. Birke: CB acknowledges the support by the German Research Foundation (DFG) under the project no. KL 566/22-1.

C. Birke (✉) · C. Klingenberg
Department of Mathematics, University of Würzburg, Würzburg, Germany
e-mail: claudius.birke@mathematik.uni-wuerzburg.de

E. Franck et al. (eds.), *Finite Volumes for Complex Applications X—Volume 2, Hyperbolic and Related Problems*, Springer Proceedings in Mathematics & Statistics 433,
https://doi.org/10.1007/978-3-031-40860-1_5

In this paper we focus only on part (a) of the first strategy, i.e. the design of the numerical flow function and for practical reasons combine it with an explicit time-stepping method. Typically, from implementing a low Mach number fix follows that the solver does not satisfy a discrete entropy inequality anymore. This is different for the two-speed relaxation technique. As already shown for isentropic Euler [3], full Euler [4] and full Euler equations with gravity [2], the resulting approximate Riemann solver reduces dissipation in the low Mach number regime and still satisfies a discrete entropy inequality. In the spirit of these papers, we apply the two-speed technique to an existing relaxation system for the ideal MHD equations [5, 6]. In a first step we show how the artificial dissipation is reduced in the low Mach number regime and substantiate this theoretical result in numerical tests. We assume that the approximate Riemann solver satisfies a discrete entropy inequality as in previous work, but do not show it here. This is left to future work.

2 MHD Equations

The compressible ideal MHD equations can be written as

$$\begin{aligned} \frac{\partial \rho}{\partial t} + \nabla \cdot (\rho \boldsymbol{U}) &= 0, \\ \frac{\partial (\rho \boldsymbol{U})}{\partial t} + \nabla \cdot [\rho \boldsymbol{U} \otimes \boldsymbol{U} + (p + \frac{1}{2}|\boldsymbol{B}|^2)\boldsymbol{I} - \boldsymbol{B} \otimes \boldsymbol{B}] &= \boldsymbol{0}, \\ \frac{\partial E}{\partial t} + \nabla \cdot [(E + p + \frac{1}{2}|\boldsymbol{B}|^2)\boldsymbol{U} - \boldsymbol{B}(\boldsymbol{B} \cdot \boldsymbol{U})] &= 0, \\ \frac{\partial \boldsymbol{B}}{\partial t} + \nabla \cdot (\boldsymbol{U} \otimes \boldsymbol{B} - \boldsymbol{B} \otimes \boldsymbol{U}) &= \boldsymbol{0}, \end{aligned} \tag{1}$$

where ρ denotes the density, $\boldsymbol{U} = (u, u_\perp)$ the velocity field, $\boldsymbol{B} = (B_x, B_\perp)$ the magnetic field and p the gas pressure. The total energy E is defined as $E = \rho e + \frac{1}{2}\rho|\boldsymbol{U}|^2 + \frac{1}{2}|\boldsymbol{B}|^2$, where e denotes the specific internal energy. The system is closed by an equation of state, which provides the numerical value of the gas pressure. Throughout this work we will consider an ideal gas law defined by $p(\rho, e) = (\gamma - 1)\rho e$. In addition to the set of equations in (1), the magnetic field satisfies the solenoidal constraint $\nabla \cdot \boldsymbol{B} = 0$. Solutions to the system (1) automatically satisfy this condition at all times if the initial field obeys the constraint.

In order to analyze the behaviour of solutions in the low Mach number regime it is of help to determine the dimensionless form of the MHD equations.

$$
\begin{aligned}
\frac{\partial \hat{\rho}}{\partial \hat{t}} + \hat{\nabla} \cdot (\hat{\rho}\hat{\boldsymbol{U}}) &= 0, \\
\frac{\partial (\hat{\rho}\hat{\boldsymbol{U}})}{\partial \hat{t}} + \hat{\nabla} \cdot \left[\hat{\rho}\hat{\boldsymbol{U}} \otimes \hat{\boldsymbol{U}} + \left(\frac{\hat{p}}{\hat{\mathcal{M}}_{\text{son}}^2} + \frac{1}{\hat{\mathcal{M}}_{\text{Alf}}^2} \frac{1}{2} |\hat{\boldsymbol{B}}|^2 \right) \boldsymbol{I} - \frac{\hat{\boldsymbol{B}} \otimes \hat{\boldsymbol{B}}}{\hat{\mathcal{M}}_{\text{Alf}}^2} \right] &= \boldsymbol{0}, \\
\frac{\partial (\hat{\rho}\hat{E})}{\partial \hat{t}} + \hat{\nabla} \cdot \left[\left(\hat{\rho}\hat{E} + \hat{p} + \frac{\hat{\mathcal{M}}_{\text{son}}^2}{\hat{\mathcal{M}}_{\text{Alf}}^2} \frac{1}{2} |\hat{\boldsymbol{B}}|^2 \right) \hat{\boldsymbol{U}} - \hat{\boldsymbol{B}} \left(\hat{\boldsymbol{B}} \cdot \hat{\boldsymbol{U}} \right) \frac{\hat{\mathcal{M}}_{\text{son}}^2}{\hat{\mathcal{M}}_{\text{Alf}}^2} \right] &= 0, \\
\frac{\partial \hat{\boldsymbol{B}}}{\partial \hat{t}} + \hat{\nabla} \cdot (\hat{\boldsymbol{U}} \otimes \hat{\boldsymbol{B}} - \hat{\boldsymbol{B}} \otimes \hat{\boldsymbol{U}}) &= \boldsymbol{0},
\end{aligned}
\tag{2}
$$

The different variables have been rescaled by some reference quantity representative of the physical system of interest: $t = t_r \hat{t}$, $x = x_r \hat{x}$, $\rho = \rho_r \hat{\rho}$, $\boldsymbol{U} = U_r \hat{\boldsymbol{U}}$, $E = a_r^2 \hat{E}$, $p = a_r^2 \hat{p}$, $\boldsymbol{B} = B_r \hat{\boldsymbol{B}}$, $a_r^2 = p_r/\rho_r$. $\hat{\mathcal{M}}_{\text{son}} = |U_r|/a_r$ and $\hat{\mathcal{M}}_{\text{Alf}} = |U_r|/(|B_r|/\sqrt{\rho_r})$ represent the characteristic sonic and Alfvén Mach numbers of the flow. The system (2) has seven eigenvalues, which can be expressed using the normal vector $\boldsymbol{n}$ by

$$
\lambda_{1,7} = \hat{\boldsymbol{U}} \cdot \boldsymbol{n} \mp c_{\text{f}}, \;\; \lambda_{2,6} = \hat{\boldsymbol{U}} \cdot \boldsymbol{n} \mp c_{\text{A}}, \;\; \lambda_{3,5} = \hat{\boldsymbol{U}} \cdot \boldsymbol{n} \mp c_{\text{s}}, \;\; \lambda_4 = \hat{\boldsymbol{U}} \cdot \boldsymbol{n}. \tag{3}
$$

The fast and slow magnetosonic and Alfvén wave speeds are defined by

$$
c_{\text{f,s}} = \left[\frac{1}{2} \left(a^2 + \frac{1}{\hat{\mathcal{M}}_{\text{Alf}}} \frac{|\hat{\boldsymbol{B}}|^2}{\hat{\rho}} \pm \sqrt{\left(a^2 + \frac{1}{\hat{\mathcal{M}}_{\text{Alf}}} \frac{|\hat{\boldsymbol{B}}|^2}{\hat{\rho}} \right)^2 - 4a^2 c_{\text{A}}^2} \right) \right]^{\frac{1}{2}}, \tag{4}
$$

$$
c_{\text{A}} = \frac{1}{\hat{\mathcal{M}}_{\text{Alf}}} \frac{|\hat{\boldsymbol{B}} \cdot \boldsymbol{n}|}{\sqrt{\hat{\rho}}}, \tag{5}
$$

with the sound speed $a = \frac{1}{\hat{\mathcal{M}}_{\text{son}}} \sqrt{\frac{\gamma \hat{p}}{\hat{\rho}}}$. Note that adding the root term in (4) results in the fast wave speed c_{f} while subtracting it in the slow wave speed c_{s}. In this work we only consider low sonic Mach numbers, but not low Alfvén Mach numbers. Therefore, we set $\hat{\mathcal{M}}_{\text{Alf}} = 1$ in the rest of the paper.

3 Relaxation Model

Our goal is to derive a one-dimensional Riemann solver. Therefore, in the following we only consider one spatial dimension. In [5, 6] a relaxation system is described, which leads to a 5-wave approximate Riemann solver for the MHD equations. For problems with low Mach numbers, however, this solver introduces excessive dissipation, so that the solution is poorly resolved on coarse grids (see Sect. 5). To cure this defect, we reformulate this relaxation system using a two-speed relaxation technique [3, 4]. The resulting system writes

$$
\begin{aligned}
\partial_t \rho + \partial_x (\rho v) &= 0, \\
\partial_t (\rho u) + \partial_x (\rho u v + \pi) &= 0, \\
\partial_t (\rho u_\perp) + \partial_x (\rho u_\perp v + \pi_\perp) &= 0, \\
\partial_t E + \partial_x \left((E + \pi) v + \pi_\perp \cdot u_\perp \right) &= 0, \\
\partial_t B_x + v \partial B_x &= 0, \\
\partial_t B_\perp + \partial_x \left(B_\perp v - B_x u_\perp \right) + u_\perp \partial_x B_x &= 0, \\
\partial_t (\rho \pi) + \partial_x \left(\rho \pi v \right) + c_1 c_2 \partial_x v &= \rho \frac{p + |B_\perp|^2/2 - B_x^2/2 - \pi}{\varepsilon}, \\
\partial_t (\rho \pi_\perp) + \partial_x \left(\rho \pi_\perp v \right) + c_a^2 \partial_x u_\perp &= \rho \frac{-B_x B_\perp - \pi_\perp}{\varepsilon}, \\
\partial_t (\rho v) + \partial_x \left(\rho v^2 \right) + \frac{c_1}{c_2} \partial_x \pi &= \rho \frac{u - v}{\varepsilon}, \\
\partial_t c_1 + v \partial_x c_1 &= 0, \\
\partial_t c_2 + v \partial_x c_2 &= 0, \\
\partial_t c_a + v \partial_x c_a &= 0,
\end{aligned}
\tag{6}
$$

where the pressure variables π and $\pi_\perp$ are defined in relaxation equilibrium by

$$
\pi = p + \frac{1}{2} |B_\perp|^2 - \frac{1}{2} B_x^2 \quad \text{and} \quad \pi_\perp = -B_x B_\perp. \tag{7}
$$

In this two-speed approach the relaxation speed for the normal direction is split into two different speeds and additionally a new relaxation equation for the velocity is introduced. At this point we would like to point out that the relaxation system (6) has a total number of three relaxation speeds (c_1, c_2 and c_a), but that we always refer to c_1 and c_2 when using the term *two-speed*.

As long as the relaxation speeds c_1, c_2 and c_a satisfy the stability conditions

$$
\begin{aligned}
\frac{1}{\rho} - \frac{B_x^2}{c_a^2} \geq 0, \quad c_1 c_2 - \rho^2 a^2 \geq 0, \\
|B_\perp| \leq (c_1 c_2 - \rho^2 a^2) \left(\frac{1}{\rho} - \frac{B_x^2}{c_a^2} \right), \quad c_1 \geq c_2,
\end{aligned}
\tag{8}
$$

solutions of the relaxation system are viscous approximations of the solutions of the original MHD system. The conditions in (8) are the result of a Chapman-Enskog expansion for the relaxation system (6) that follows the same steps as the one for the one-speed system in [5]. The homogeneous system $(6)_{\varepsilon=\infty}$ is hyperbolic and admits 5 different eigenvalues

$$
\lambda_1 = v - \frac{c_1}{\rho}, \quad \lambda_2 = v - \frac{c_a}{\rho}, \quad \lambda_3 = v \quad \lambda_4 = v + \frac{c_a}{\rho} \quad \lambda_5 = v + \frac{c_1}{\rho}, \tag{9}
$$

where the eigenvalue v has multiplicity 8. All characteristic fields are linearly degenerate and the Riemann invariants for the different waves are given as follows

$$
\begin{aligned}
v-\frac{c_1}{\rho}:\ & v-\frac{c_1}{\rho},\ u-\frac{c_2}{\rho},\ \pi+\frac{c_1c_2}{\rho},\ \frac{B_\perp}{\rho}, u_\perp,\ B_x,\ \pi_\perp,\ c_1,\ c_2,\ c_a,\\
& \frac{2c_1c_2-c_2^2-2c_2\rho(v-u)+\rho\left(2\pi+|B_\perp|^2+B_x^2+2\rho e\right)}{2\rho^2},\\
v-\frac{c_a}{\rho}:\ & \pi_\perp+c_au_\perp,\ B_\perp-\frac{\rho u_\perp B_x}{c_a},\ e+\frac{c_a^2u_\perp^2+2c_au_\perp(B_xB_\perp+\pi_\perp)-\rho B_x^2u_\perp^2}{2c_a^2},\\
& \rho,\ u,\ B_x,\ \pi,\ v,\ c_1,\ c_2,\ c_a,\\
v:\ & v,\ u_\perp,\ \pi,\ \pi_\perp,\\
v+\frac{c_a}{\rho}:\ & \pi_\perp-c_au_\perp,\ B_\perp+\frac{\rho u_\perp B_x}{c_a},\ e+\frac{c_a^2u_\perp^2-2c_au_\perp(B_xB_\perp+\pi_\perp)-\rho B_x^2u_\perp^2}{2c_a^2},\\
& \rho,\ u,\ B_x,\ \pi,\ v,\ c_1,\ c_2,\ c_a,\\
v+\frac{c_1}{\rho}:\ & v+\frac{c_1}{\rho},\ u+\frac{c_2}{\rho},\ \pi+\frac{c_1c_2}{\rho},\ \frac{B_\perp}{\rho},\ u_\perp,\ B_x,\ \pi_\perp,\ c_1,\ c_2,\ c_a,\\
& \frac{2c_1c_2-c_2^2+2c_2\rho(v-u)+\rho\left(2\pi+|B_\perp|^2+B_x^2+2\rho e\right)}{2\rho^2}.
\end{aligned}
$$

Let us now introduce the state vector

$$W=(\rho,\rho u,\rho u_\perp,E,B_x,B_\perp,\rho\pi,\rho\pi_\perp,\rho v,c_1,c_2,c_a)^T. \tag{10}$$

The solution to the Riemann problem associated with system $(6)_{\varepsilon=\infty}$ given by

$$W_0(x)=\begin{cases}W^L, & x<0,\\ W^R, & x>0,\end{cases} \tag{11}$$

consists of six constant states. Therefore the Riemann solver $W_{\mathcal{R}}(x/t;W^L,W^R)$ has the structure

$$W_{\mathcal{R}}(x/t;W^L,W^R)=\begin{cases}W^L, & \frac{x}{t}<\min(\lambda_1,\lambda_2),\\ W^{L*}, & \min(\lambda_1,\lambda_2)<\frac{x}{t}<\max(\lambda_1,\lambda_2),\\ W^{L**}, & \max(\lambda_1,\lambda_2)<\frac{x}{t}<\lambda_3,\\ W^{R**}, & \lambda_3<\frac{x}{t}<\min(\lambda_4,\lambda_5),\\ W^{R*}, & \min(\lambda_4,\lambda_5)<\frac{x}{t}<\max(\lambda_4,\lambda_5),\\ W^R, & \max(\lambda_4,\lambda_5)<\frac{x}{t}.\end{cases} \tag{12}$$

The intermediate states can be derived using the invariants from above. Since each Riemann invariant is constant accross its corresponding wave, the invariants pose a

system of equations that can be solved for the intermediate states. Due to their large number, we will not list the intermediate states here. The definition of the relaxation speeds is given in Sect. 4.

4 Definition of the Relaxation Speeds and the Low Mach Number Property

Starting from the stability conditions in (8), the relaxation speeds for the two-speed solver can be derived with steps very similar to those in [6] for $k = 1, 2$:

$$\begin{aligned} c_k^L &= \rho^L a_{0,k}^L + \beta\rho^L \left((v^L - v^R)_+ + \frac{(\pi^R - \pi^L)_+}{\rho^L a_q^L + \rho^R a_q^R} \right), \\ c_k^R &= \rho^R a_{0,k}^R + \beta\rho^R \left((v^L - v^R)_+ + \frac{(\pi^L - \pi^R)_+}{\rho^L a_q^L + \rho^R a_q^R} \right), \\ c_a^L &= \sqrt{\frac{\rho^L}{x^L} \left((B_x^L)^2 + |B_x^L B_\perp^L| \right)}, \quad c_a^R = \sqrt{\frac{\rho^R}{x^R} \left((B_x^R)^2 + |B_x^R B_\perp^R| \right)}, \end{aligned} \tag{13}$$

with

$$a_{0,1}^2 = \frac{1}{\min\left(\phi^2, 1\right)} a^2 + \frac{|B_\perp|^2 + |B_x B_\perp|}{\rho x}, \tag{14}$$

$$a_{0,2}^2 = \min\left(\phi^2, 1\right) a^2 + \frac{|B_\perp|^2 + |B_x B_\perp|}{\rho x}, \tag{15}$$

$$a_q^2 = \min\left(\phi^2, 1\right) a^2 + \frac{|B_\perp|^2 + |B_x B_\perp|}{\rho}. \tag{16}$$

For more details on the definitions of the used quantities, we refer the reader to [6]. We want to point out that for $\phi = 1$, we get $c_1 = c_2$ and consequently the speeds coincide with the definitions in the one-speed solver. However, to get the desired effect of the two-speed approach, we set $\phi = \hat{\mathcal{M}}_{\text{son}}$. As a consequence, taking into account the results of Sect. 2, the speeds scale in this case by

$$c_1 = \mathcal{O}(1/\hat{\mathcal{M}}_{\text{son}}^2) \quad \text{and} \quad c_2 = \mathcal{O}(1). \tag{17}$$

The rescaling by the Mach number in (14)–(16) is essential to prevent excessive numerical dissipation in the low Mach number regime. This becomes clear when looking at the intermediate state of the pressure π given by

$$\pi^* = \frac{c_2^R \pi^L + c_2^L \pi^R - c_2^L c_2^R (v^R - v^L)}{c_2^L + c_2^R}. \tag{18}$$

This state can be viewed as a central flux of the left and right pressure combined with a dissipation term including the velocity difference $v^R - v^L$. Thanks to the rescaling, c_2 is of order $\mathcal{O}(1)$, which keeps the amount of dissipation in the pressure independent of the Mach number. For the one-speed solver, on the other hand, the relaxation speed $c = c_1 = c_2$ scales with $\mathcal{O}(1/\hat{\mathcal{M}}_{son})$. Thus, in the low Mach number regime, the dissipation term becomes the dominant part of the momentum flux, causing the dissipation to increase with decreasing Mach number. The rescaling in the two-speed approach prevents this behaviour.

5 Numerical Results

The one-dimensional approximate Riemann solver (12) is incorporated into a second order two-dimensional unsplit finite volume method, that uses a standard linear reconstruction with minmod-limiter. By applying the Riemann solver separately in both spatial directions, the reduced dissipation in the low Mach number regime due to the two-speed approach is inherited by the overall scheme. In order to keep the divergence of the magnetic field to machine precision, the scheme is combined with a second order staggered constrained transport method [9]. For time discretisation, the explicit method of Heun is used under the CFL condition

$$\Delta t \leq \frac{\mathrm{CFL}}{4} \frac{\min(\Delta x, \Delta y)}{\max_i(|\lambda_i|)} \quad \text{with} \quad \mathrm{CFL} = 0.9. \tag{19}$$

For comparison, we also show results of the one-speed solver, in which the relaxation speeds are not rescaled with the Mach number and thus we set $c_1 = c_2$.

5.1 Stationary Vortex

We start with a stationary version of the Balsara vortex that can be set up with different maximum Mach numbers [1]. We compute the numerical solution on a 64×64 grid and evaluate the distribution of the local Mach number $\mathcal{M}_{loc} = |\boldsymbol{U}|/a$ relative to the maximum Mach number $\mathcal{M}_{max}$ in the initial data. The results for different $\mathcal{M}_{max}$ after one turn of the vortex ($t_f = 5.9055/\mathcal{M}_{max}$) are shown in Fig. 1. Clearly, the one-speed solver introduces too much artificial dissipation, so that the vortex is not resolved accurately for smaller Mach numbers. With the two-speed method, on the other hand, the dissipation is independent of the Mach number. This advantage is paid for by a smaller timestep in comparison to the one-speed method, since the rescaling of c_1 increases the fastest wave speed in the CFL condition.

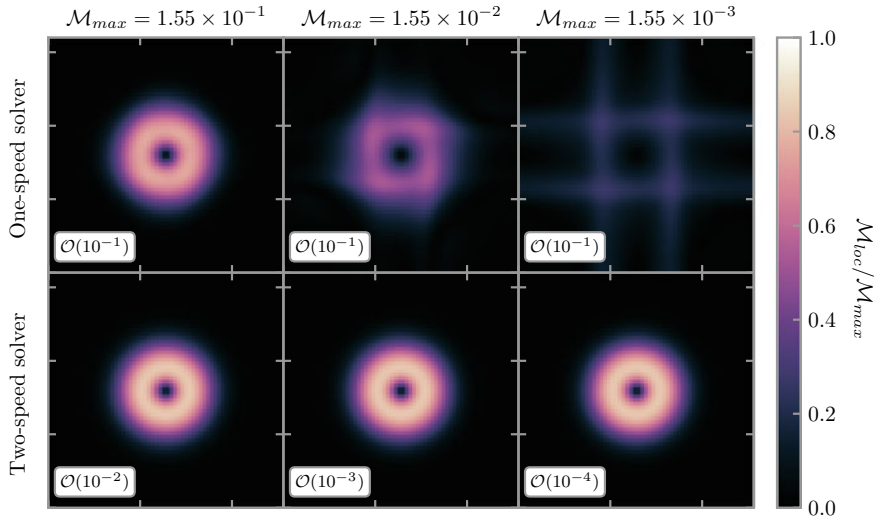

Fig. 1 Distribution of the local sonic Mach number relative to $\mathcal{M}_{max}$ after one turn on a 64×64 grid. The value in the white box gives the order of the timestep

5.2 *Kelvin Helmholtz Instability*

A more sophisticated test is the magnetised version of the Kelvin Helmholtz instability [10]. This test is set up with different maximum Mach number of the initial horizontal flow denoted by $\mathcal{M}_x$. We compute the solution on a 128×64 grid until the final time $t_f = 0.8/\mathcal{M}_x$. Figure 2 shows the distribution of the local sonic Mach

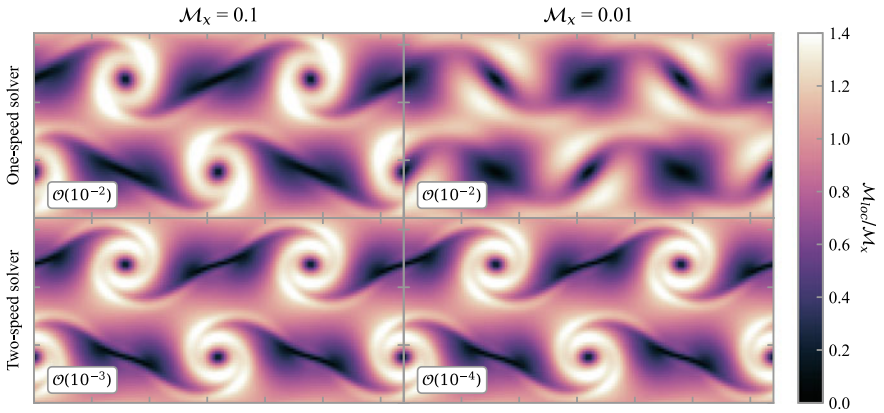

Fig. 2 Distribution of the local sonic Mach number relative to $\mathcal{M}_x$ at time t_f on a 128×64 grid. The value in the white box gives the order of the timestep

number $\mathcal{M}_{loc}$ relative to $\mathcal{M}_x$. The test again shows that the two-speed solver introduces significantly less numerical dissipation and can therefore resolve the details of the solution much better.

6 Summary

In this work, we have built an approximate Riemann solver using the two-speed technique, which gives accurate solutions even in the low Mach number regime. Typically, relaxation-based Riemann solvers satisfy a discrete entropy inequality when the subcharacteristic condition is satisfied. The goal of future work will be to prove such a result for the solver described here. Furthermore, it would be interesting to investigate whether the two-speed approach can also be applied or extended to the low Alfvén Mach number regime.

References

1. Berberich, J.P., Chandrashekar, P., Klingenberg, C.: High order well-balanced finite volume methods for multi-dimensional systems of hyperbolic balance laws. Comput. Fluids **219**, 104858 (2021)
2. Birke, C., Chalons, C., Klingenberg, C.: A low Mach two-speed relaxation scheme for the compressible Euler equations with gravity (2023). arXiv:2112.02986v3
3. Bouchut, F., Chalons, C., Guisset, S.: An entropy satisfying two-speed relaxation system for the barotropic Euler equations: application to the numerical approximation of low Mach number flows. Numerische Mathematik **145**, 35–76 (2020)
4. Bouchut, F., Franck, E., Navoret, L.: A low cost semi-implicit low-Mach relaxation scheme for the full Euler equations. J. Sci. Comput. **83**(1), 24 (2020)
5. Bouchut, F., Klingenberg, C., Waagan, K.: A multiwave approximate Riemann solver for ideal MHD based on relaxation. I: theoretical framework. Numerische Mathematik **108**, 7–42 (2007)
6. Bouchut, F., Klingenberg, C., Waagan, K.: A multiwave approximate Riemann solver for ideal MHD based on relaxation II: numerical implementation with 3 and 5 waves. Numerische Mathematik **115**, 647–679 (2010)
7. Chen, W., Wu, K., Xiong, T.: High order asymptotic preserving finite difference WENO schemes with constrained transport for MHD equations in all Sonic Mach numbers (2022). arXiv:2211.16655
8. Dumbser, M., Balsara, D.S., Tavelli, M., Fambri, F.: A divergence-free semi-implicit finite volume scheme for ideal, viscous, and resistive magnetohydrodynamics. Int. J. Numer. Methods Fluids **89**(1–2), 16–42 (2019)
9. Gardiner, T.A., Stone, J.M.: An unsplit Godunov method for ideal MHD via constrained transport. J. Comput. Phys. **205**(2), 509–539 (2005)
10. Leidi, G., Birke, C., Andrassy, R., Higl, J., Edelmann, P.V.F., Wiest, G., Klingenberg, C., Röpke, F.K.: A finite-volume scheme for modeling compressible magnetohydrodynamic flows at low Mach numbers in stellar interiors. Astron. Astrophys. **668**(A143) (2022)
11. Minoshima, T., Miyoshi, T.: A low-dissipation HLLD approximate Riemann solver for a very wide range of Mach numbers. J. Comput. Phys. **446**, 110639 (2021)